TISSUE ENGINEERING: Part A
Volume 24, Numbers 11 and 12, 2018

DOI: 10.1089/ten.tea.2017.0237

termis
Tissue Engineering
& Regenerative Medicine
International Society

ORIGINAL ARTICLE

Maintaining Elastogenicity of Mesenchymal Stem Cell-Derived Smooth Muscle Cells in Two-Dimensional Culture

Shataakshi Dahal, BE,[1] Thomas Broekelman, MS,[2] Robert P. Mecham, PhD,[2] and Anand Ramamurthi, PhD[1,3]

Abdominal aortic aneurysms (AAAs) are localized expansions of the abdominal aorta that grow slowly to rupture. AAA growth is driven by irreversible elastic matrix breakdown in the aorta wall by chronically upregulated matrix metalloproteases (MMPs). Since adult vascular smooth muscle cells (SMCs) poorly regenerate elastic matrix, we previously explored utility of bone marrow mesenchymal stem cells and SMCs derived therefrom (BM-SMCs) for this purpose. One specific differentiated phenotype (cBM-SMCs) generated on a fibronectin substrate in presence of exogenous transforming growth factor-β and platelet-derived growth factor exhibited superior elastogenicity versus other phenotypes, and usefully provided proelastogenic and antiproteolytic stimuli to aneurysmal SMCs. Since *in vivo* cell therapy demands large cell inoculates, these derived SMCs must be propagated *in vitro* while maintaining their superior elastogenic, proelastogenic, and antiproteolytic characteristics. In this work, we thus investigated the culture conditions that must be provided to this propagation phase, which ensure that the differentiated SMCs maintain their phenotype and matrix regenerative benefits. Our results indicate that our BM-SMCs retain their phenotype in long-term culture even in the absence of differentiation growth factors and fibronectin substrate, but these conditions must be continued to be provided during postdifferentiation propagation if they are to maintain their superior elastic matrix deposition, crosslinking, and fiber formation properties. Our study, however, showed that cells propagated under these conditions exhibit higher expression of MMP-2, but favorably, no expression of elastolytic MMP-9. Hence, the study outcomes provide crucial guidelines to maintain phenotypic stability of cBM-SMCs during their propagation in two-dimensional culture before their delivery to the AAA wall for therapy.

Keywords: elastic matrix, smooth muscle cells, stem cells, aortic aneurysms, regenerative repair

Introduction

Abdominal aortic aneurysms (AAAs) are localized expansions of the abdominal aorta that slowly grow to a rupture-prone stage. AAAs develop due to slow proteolytic degradation of wall structural proteins, collagen, and elastic fibers by chronically upregulated enzymes and the matrix metalloproteases (MMPs) MMP-2 and MMP-9 in particular.[1,2] These enzymes are associated with chronic transmural inflammation, and depletion[3] and phenotypic switch of vascular smooth muscle cells (SMCs) to a diseased state.[4] AAAs primarily afflict the elderly, with male smokers at high risk.[3] Current treatment options for AAAs are surgical, but are performed mostly only on large, rupture-prone AAAs bigger than the critical size (maximal diameter >5.5 cm) and have high procedural risk for many older AAA patients.[5–7] Alternative nonsurgical treatments to slow, arrest, or even regress small AAAs during their slow (>5 years) growth to rupture are thus mandated.

A critical requirement to be able to arrest or regress AAA growth is to restore homeostasis of the structural extracellular matrix (ECM) in the AAA wall. Elastic fibers and higher order structures (elastic lamellae) in the aorta wall, which enable vessel stretch and recoil, are unlike collagen in not being able to autoregenerate or repair postdisruption, in adults.[8] In the light of chronic matrix breakdown in the

[1]Department of Biomedical Engineering, Cleveland Clinic, Cleveland, Ohio.
[2]Department of Cell Biology and Physiology, Washington University at St. Louis, St. Louis, Missouri.
[3]Department of Molecular Medicine, Cleveland Clinic Lerner College of Medicine of Case Western Reserve University, Cleveland, Ohio.

AAA wall, it is imperative to provide a major impetus to elastic matrix neoassembly (elastogenesis) concurrent with a deterrent to enzymatic proteolysis, so as to allow for net accumulation of new elastic matrix. Based on literature describing the role of stem cells in developmental elastogenesis and vascular tissue repair postinjury,[9] in a prior cell culture study,[10] we showed that SMC-like progenitor cells (BM-SMCs) derived from bone marrow mesenchymal stem cells (BM-MSCs) exhibit significantly higher elastogenic capacity than healthy, terminally differentiated adult vascular SMCs and are able to stimulate elastic matrix neoassembly by aneurysmal SMCs, and in parallel attenuate MMP-mediated elastic matrix breakdown. We subsequently demonstrated that these effects of BM-SMCs in stimulating elastic fiber formation, elastin crosslinking, and attenuating MMP activity by aneurysmal SMCs are (1) not provided by undifferentiated BM-MSCs,[10] and (2) mediated by biological factors contained in paracrine secretions (secretome) of the BM-SMCs.[10]

SMCs represent a continuum of phenotypic states that span between extreme, but theoretical phenotypes of quiescent, highly contractile, and nonsynthetic cells (''contractile phenotype'') and a highly proliferative, robustly ECM-generating, and poorly contractile state (''synthetic phenotype''), respectively.[11,12] While high contractility of terminally differentiated SMCs resident in adult blood vessels allows the vessel to effectively maintain blood pressure, robust ECM synthesis by SMCs in developing vascular tissues and in the injured vascular wall contributes to vascular tissue organization and remodeling/repair, respectively.[13] However, most SMCs represent interim phenotypes that can exhibit aspects of both phenotypic extremes.[11,12] In this context, in prior work,[14] we demonstrated that phenotypic coordinates of derived BM-SMCs can be altered by modulating conditions of differentiation culture and represent a useful metric to select cells exhibiting superior elastogenicity, contractility, and sufficient proliferative capacity for successful application to regenerative AAA repair.

We identified a specific BM-SMC phenotype we now term as cBM-SMCs, which were derived from rat BM-MSCs on a fibronectin (Fn) substrate in the presence of Dulbecco's modified Eagle's medium (DMEM)-F12 containing 10% fetal bovine serum (FBS), transforming growth factor-beta (TGF-β1; 2.5 ng/mL), and platelet-derived growth factor-ββ (PDGF-ββ; 5 ng/mL) that exhibited superior properties consistent with that listed above. Cell therapy demands large cell inoculates, which in turn necessitates that the differentiated cells be propagated in culture before delivery to the collagenous, de-elasticized vascular tissue *in vivo*. While we have confirmed, in a parallel study, that our differentiated cells maintain their phenotype and functional benefits to aneurysmal SMCs in such a 3D tissue milieu, when cultured in the absence of any of the differentiation growth factors or Fn, we also sought to understand how conditions of postdifferentiation *in vitro* 2D culture for the purpose of propagating cBM-SMCs for subsequent *in vivo* use impact their phenotypic, functional, and matrix regenerative properties. This latter aspect was investigated in this study.

Materials and Methods

Propagation of rBM-SMCs and cBM-SMCs

Rat BM-MSCs (Invitrogen, Carlsbad, CA) were differentiated into cBM-SMCs, as described earlier.[10] At 21 days of differentiation, the cells were trypsinized and (1) seeded on uncoated tissue culture polystyrene flasks, cultured with DMEM F-12 medium containing 10% v/v FBS (Invitrogen) and 1% v/v PenStrep (Thermo Fisher, South Logan, UT) without any growth factors (rBM-SMC), and subsequently passaged upon attaining near confluence, and (2) seeded within human fibronectin (hFN, 100 ng/mL)-coated tissue culture flasks (BD Biosciences, East Rutherford, NJ) cultured with DMEM-F12 medium containing 10% v/v FBS, 1% v/v PenStrep, 2.5 ng/mL of TGF-β1 (Peprotech), and 5 ng/mL of PDGF-ββ (Peprotech, Rocky Hill, NJ). These cells, termed cBM-SMCs, were subsequently passaged when they attained near confluence and used for further experimentation to compare their phenotypes, and retention of elastogenic and antiproteolytic effects. In these experiments, healthy rat aortic smooth muscle cells (RASMCs) and BM-MSCs were studied as controls. For transmission electron microscopy (TEM) analysis, EaRASMCs (aneurysmal rat aortic smooth muscle cells) (passage 3–5) isolated from an elastase injury rat AAA model, as we have described previously,[14] were cultured as negative controls. The propagation condition of RASMCs (used as positive control) has been previously described.[15] Briefly, the abdominal aorta of three different healthy rats were harvested, cut into small pieces, and digested in collagenase type-2 (Worthington Biochemical, Lakewood, NJ) and porcine elastase (Sigma, St. Louis, MO). These digests were then aliquoted equally in each well of 6-well plate and cultured in DMEM containing 20% v/v FBS and 1% v/v PenStrep for SMC isolation. Once the primary cells adhered and reached confluence, they were passaged and cultured in media containing 10% v/v FBS. Passage 2 RASMCs generated from the three different animals were then pooled, passaged, and seeded for culture experiments.

RNA isolation and real-time polymerase chain reaction

The rBM-SMCs were seeded in polystyrene 6-well plates (USA Scientific, Ocala, FL) and cBM-SMCs were seeded in human Fn-coated 6-well plates (BD Biosciences) at 15,000 cells per well ($A = 10\,cm^2$) and cultured for 15 days. Total RNA was isolated from the cultures using an RNeasy mini kit (Qiagen, Valencia, CA) and quantified using a Quant-iT™ Ribogreen® RNA kit (Invitrogen) following manufacturer's instructions. An iScript cDNA synthesis kit (Bio-Rad, Hercules, CA) was used to synthesize cDNA using 1 μg of RNA from all the samples and reverse transcription was performed for a total of 40 min combining 5 min at 25°C, 30 min at 42°C, and 5 min at 85°C according to the manufacturer's instructions. Real-time polymerase chain reaction (PCR) was performed using an Applied Biosystems 7500 Real-Time PCR system with Power SYBR® Green Master Mix (Applied Biosystems). Specially designed primers were used for the *18s* (housekeeping gene), α-SMA (*ACTA 2*), caldesmon (*CALD1*), smoothelin (*SMTN*), smooth muscle myosin heavy chain (*MYH11*), elastin (*ELN*), fibrillin-1 (*FBN1*), fibulin-4 (*FBLN4*), fibulin-5 (*FBLN5*), lysyl oxidase (*LOX*), MMP-2 (*MMP2*), MMP-9 (*MMP9*), and Timp-1 (*TIMP1*). The primers were designed previously in our laboratory.[9,15,16] The PCR data were analyzed using LinReg PCR program. This program uses a MATLAB® code separately for each sample to determine the baseline-corrected set of values and window of linearity. PCR efficiency was calculated from the slope of linear

fit for each sample. This provided correction for N0. Data value obtained from this analysis was directly used to calculate gene expression ratio as described in literature.[17]

Immunofluorescence-based detection of SMC phenotypic markers and elastic matrix homeostasis proteins

SMC markers and key proteins involved in elastic fiber hemostasis were detected using immunofluorescence (IF) staining, as described previously.[18] Cells were seeded on coverslips, cultured for 7 days for SMC marker proteins and 21 days for elastin homeostasis proteins, then were fixed using 4% w/v paraformaldehyde for 20 min at 4°C, permeabilized with 0.1% v/v Triton X-100 (VWR Scientific, West Chester, PA) for 10 min, and blocked with phosphate-buffered saline (PBS) containing 5% v/v goat serum (Gibco Life Technologies, Grand Island, NY). The cells were then incubated overnight with primary antibodies against the SMC marker proteins (caldesmon, α-SMA, smoothelin, and myosin heavy chain [MHC]) and elastin homeostasis proteins (elastin, fibrillin-1, fibulin-4, fibulin-5, LOX, MMP-2, MMP-9, and TIMP-1). The expression of these proteins was then visualized using secondary antibodies conjugated to AlexaFluor 488 or 633 probes (Molecular Probes, Temecula, CA). The coverslips were then mounted on glass slide with Vectashield® mounting medium containing the nuclear dye, 4′,6-Diamidine-2′-phenylindole dihydrochloride (DAPI) (Vector Labs, Burlingame, CA). Imaging was done using Olympus I×51 fluorescence microscope (Olympus, Pittsburgh, PA) and the images were analyzed using Image Pro® software.

DNA assay for cell proliferation

DNA content in the cells were quantified using Hoechst Dye Based Fluorometric DNA assay protocol as described earlier.[14] The cell layers at 21 days of culture were harvested in Pi buffer (50 mM Na_2HPO_4, 2 mM EDTA, and 0.3 mM NaN_3) and sonicated to lyse cells and release DNA. The results were quantified assuming 6 pg of DNA contained per cell.

Fastin assay for matrix elastin

At 21 days of culture, the cell layers were harvested in Pi buffer and sonicated. A 0.5 mL aliquot of the sonicated cell layer samples was digested in 0.1 mL of 1.5 M oxalic acid (95°C, 90 min) and then pelleted by centrifugation at 14,000 *g*. The supernatant containing soluble α-elastin was saved and 0.4 mL of 0.25 M oxalic acid added to the pellet and digested for a further 1 h at 100°C. The digestate was centrifuged again and the supernatant pooled with the earlier supernatant fraction. The elastin content in the pooled supernatant was measured using a FASTIN® assay kit (Accurate Chemical and Scientific Corp) as per manufacturer's instructions. The measured elastin content in the samples was normalized to their corresponding DNA content.

Hydroxyproline assay for collagen matrix

A hydroxyproline (OH-Pro) assay was performed to determine the total amount of collagen deposited by the cells in their ECM as described in our published literature.[14] Briefly, the cell layers were harvested in Pi buffer, centrifuged at 2500 rpm for 10 min, and the resulting pellet digested in 1 mL of 0.1 M NaOH at 95°C in a water bath for 1 h to solubilize elastin and collagen. The digestate was then allowed to cool to room temperature and centrifuged at 2500 rpm. The supernatant containing solubilized collagen was assayed using the OH-Pro assay. Collagen amounts were calculated based on 13.5% w/w OH-Pro content of collagen.

Estimation of desmosine crosslink content

After 21 days of culture, all four cell types were harvested in PBS, pH 7.4 and centrifuged for 5 min at 500 *g* to form pellets. The cell pellets were hydrolyzed with 6 N HCl for 48 h at 105°C, evaporated to dryness, and reconstituted in 400 μL of water. The samples were then filtered through a 0.45 μm filter and desmosine levels determined using a competitive ELISA assay.[15] Total protein in each sample aliquot was measured using the ninhydrin assay.[19]

Western blot analysis

Western blot analysis was performed to semiquantitatively compare protein expression for the SMC phenotypic marker proteins α-SMA, caldesmon, smoothelin, and MHC, MMP-2, and MMP-9, tissue inhibitor of matrix metalloprotease-1 (TIMP-1), and lysyl oxidase (LOX), between the four cell types. Briefly, the cells were seeded at a density of 30,000/well in a 6-well plate ($n=6$ wells/case) and cultured for 21 days. The cell layers were harvested in RIPA buffer containing a protease inhibitor cocktail (Thermo Scientific, Waltham, MA). The amount of protein in each sample was quantified using the BCA assay kit (Thermo Scientific, Waltham, MA). Western blotting was performed as previously described.[20] Briefly, an equal volume of protein sample with protein amount within the threshold range of 20 to 30 μg in each case was taken and mixed with a loading buffer. The mixture was reduced and loaded along with a prestained molecular weight ladder (Invitrogen) on to 4–12% and 10% sodium doodecyl sulfate - polyacrylamide gel electrophoresis (SDS-PAGE) gels for molecular weight (MW) <60 kDa and MW >60 kDa proteins, respectively. The gels were subjected to dry transfer onto nitrocellulose membranes using iBlot Western Blotting system (Invitrogen). The membranes were then blocked with the Odyssey blocking buffer (LiCOR Biosciences, Lincoln, NE) for 1 h at room temperature, and then incubated overnight with respective primary antibodies for different proteins. Following this, the blots were incubated with secondary antibodies against rabbit and mouse conjugated with IRDye® 680LT (1:15,000 dilution) and IRDye 800 CW (1:20,000 dilution), respectively. The bands were observed using a LiCOR Odyssey laser-based scanning system, quantified using Image Studio Lite software, and quantified as relative density units normalized to the intensity of housekeeping protein (β-actin) bands. The advantage of β-actin over other proteins used as loading control (e.g., GADPH) is that it is expressed by all eukaryotic cell types and its expression level does not vary drastically due to cellular treatment or across tissue types.[21] For this reason, it has been adopted as a loading control by many published studies involving assessment of SMCs.[22–25]

ELISA for MMP-2 and MMP-9 proteins

Solid-phase ELISA was performed to determine the relative mass values for naturally occurring MMP-2 and MMP-9

using Quantikine® ELISA kit (Catalog No. MMP200 and MMP900, respectively; R&D Systems, Minneapolis). Briefly, all four cell types were seeded at 30,000 cells/well in a 6-well plate ($n=6$ wells/case). At 21 days of culture, they were harvested in RIPA buffer with protease inhibitor cocktail, as described above for Western blot analysis. The assay reagents and standards were prepared as per manufacturer's instructions. The assay was carried out in a 96-well plate, adding the appropriate amount of reagents followed by multiple wash steps as indicated in the manufacturer's protocol. The optical density was measured using the Cytation 5 plate reader with $\lambda=450$ nm and $\lambda=570$ nm. The absorbance values at 570 nm were subtracted from the values at 450 nm to provide corrections for optical imperfections in the plate. Concentration versus optical density graph was plotted for standard curve and log–log plot was used for final calculations.

Transmission electron microscopy

The ultrastructure of the deposited elastic matrix in all four sets of cultures was visualized using TEM, as we have previously described.[26] Briefly, following 21 days of culture on Permanox® chamber slides (Source), the cell layers were washed with 37°C PBS, fixed for 5 min at 37°C followed by overnight fixation with 2.5 w/v glutaraldehyde in 0.1 M sodium cacodylate buffer, dehydrated in a graded ethanol series (50–100% v/v), embedded in Epon 812 resin, sectioned, placed on copper grids, stained with uranyl acetate and lead citrate, and visualized on a Hitachi TEM H7600T (High technologies, Pleasanton, CA).

Statistical analysis

All experiments and analyses were performed on $n=6$ replicate cultures per cell type with the following exceptions: Western blot, $n=3$ and MMP-2 and MMP-9 ELISA, $n=3$. Results are reported as mean ± SD with statistical significance of differences determined by one way-ANOVA and deemed for a p-value of <0.05.

Results

Gene expression profiles of BM-MSCs, RASMCs, and differentiated SMC types

Results of reverse transcription (RT)-PCR analysis are presented in Figure 1. Gene expression data are shown as log-transformed values of the averages of measured relative fluorescence units (RFUs) since the expression levels differ significantly between genes and cell types, spanning several orders of magnitude. Expression of *ACTA2* was significantly higher in cBM-SMCs compared to all other cell types ($p<0.001$), whereas *CALD1* expression was significantly higher in the RASMC control ($p<0.001$); *CALD1* expression was significantly higher in rBM-SMCs versus

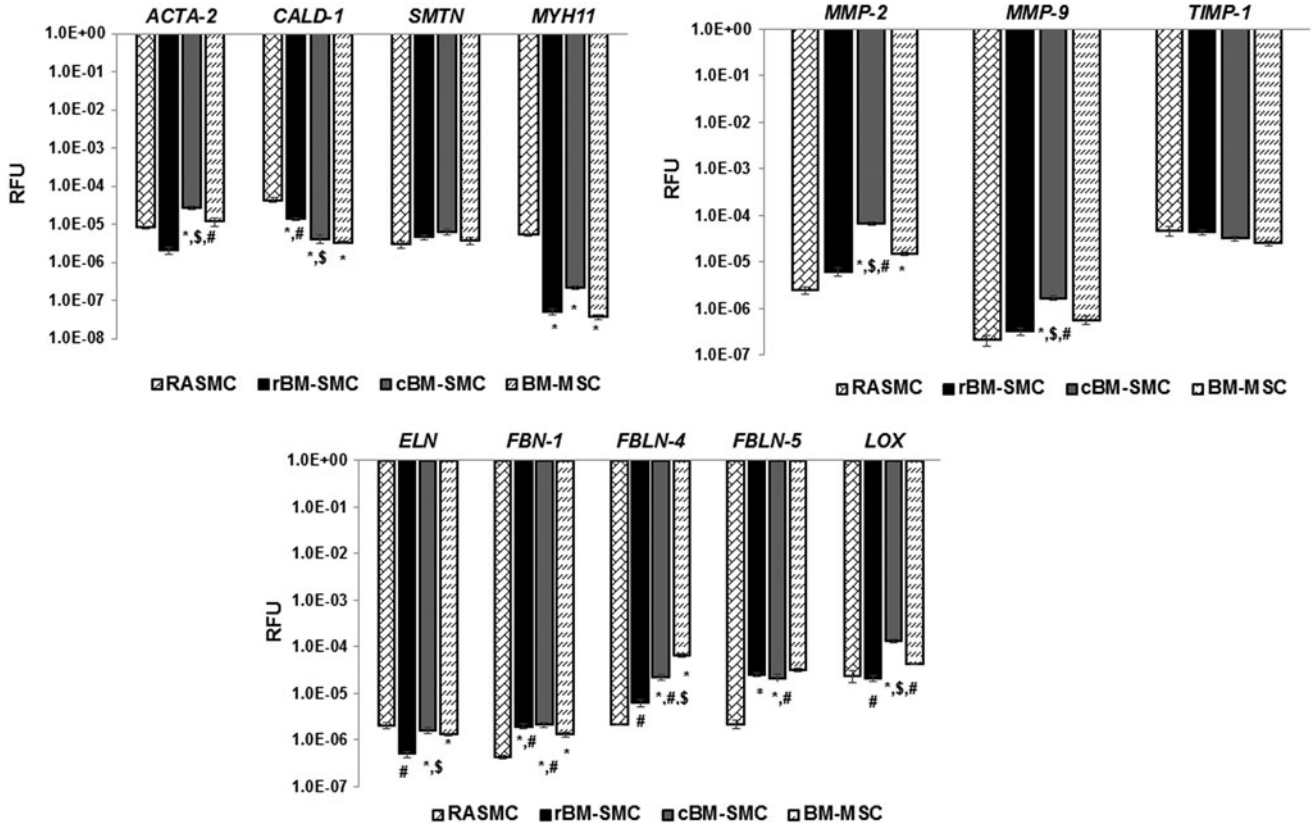

FIG. 1. Gene expression profiles for smooth muscle cell marker proteins and elastin homeostasis marker proteins. Gene expression is shown as log-transformed values of average measured RFUs. Cultures of the four different cell types were analyzed using RT-PCR at 15 days of culture. *, $, and # indicate statistical significance compared to RASMCs, cBM-SMCs, and BM-MSCs, respectively, deemed for $p<0.05$. BM-MSCs, bone marrow mesenchymal stem cells; RASMCs, rat aortic smooth muscle cell; RFUs, relative fluorescence units; SMCs, smooth muscle cell.

cBM-SMCs ($p=0.015$). *SMTN* expression was not different between the two derived SMC types. *MYH11* expression was the highest among RASMCs and significantly more so than the other cell types ($p<0.001$). There were no differences between the two derived phenotypes.

ELN expression by the cBM-SMCs was significantly higher versus rBM-SMCs ($p<0.001$). *ELN* expression by the rBM-SMCs was lower than even BM-MSCs ($p=0.002$). Expression of *FBN1* was significantly higher in both the derived phenotypes compared to RASMCs ($p<0.001$) and BM-MSCs ($p<0.05$), although there were no differences between them. *FBLN4* expression was significantly higher in cBM-SMC cultures ($p=0.003$) than in RASMC cultures and rBM-SMC cultures ($p=0.007$), and even more so in BM-MSC cultures. *FBLN4* expression in the BM-MSC cultures was significantly higher than both cBM-SMCs. *FBLN5* expression was significantly higher ($p<0.05$) in cBM-SMC cultures versus RASMCs and BM-MSCs, but was not different from the rBM-SMCs. *LOX* expression was significantly higher in cBM-SMC cultures relative all other cell groups ($p<0.001$), as also expression of *MMP2* and *MMP9* genes ($p<0.01$). TIMP-1 expression was similar in all cell types.

Expression of SMC phenotypic marker proteins and elastin homeostasis proteins

Results of Western blot analyses are presented in Figure 2. Despite apparent differences, expression levels of key SMC marker proteins (caldesmon, α-SMA, smoothelin, and MHC) were not significantly different between the cell groups. Expression of key proteins involved in elastic fiber homeostasis, namely LOX, fibulin-4, and fibulin-5 were significantly higher in cBM-SMC cultures than in all other cell groups ($p\leq0.001$, $p\leq0.005$, and $p\leq0.01$, respectively). TIMP-1 expression was similar in all groups.

As shown in Figure 3, total MMP-2 protein synthesis was significantly higher in cBM-SMC cultures compared to RASMCs ($p<0.001$), rBM-SMCs, ($p<0.001$) and BM-MSCs ($p=0.006$) Expression of the active MMP-2 isoform was again the highest in cBM-SMC cultures ($p<0.001$ vs. other groups), followed by the rBM-SMCs ($p=0.002$ vs. RASMC and $p=0.039$ vs. BM-MSCs). Expression ratios of active MMP-2 to TIMP-1 were significantly higher in cBM-SMC cultures than in RASMC cultures ($p=0.03$), but were found to be not different versus rBM-SMCs and BM-MSCs. MMP-9 was not detected on the Western blots. The results of IF (Supplementary Fig. S1; Supplementary Data are available online at www.liebertpub.com/tea) also qualitatively represent and validate the amount of expression of these SMC markers and elastin homeostasis proteins.

Cell proliferation

A DNA assay showed an increase in DNA content (i.e., number of cells) over 21 days to be significantly lower in the derived cell types (and RASMCs) relative to BM-MSCs ($p<0.001$) and significantly higher versus RASMCs ($p<0.001$) (Fig. 4A). There were no differences in cell proliferation between the rBM-SMCs and cBM-SMCs.

Elastic matrix synthesis

Figure 4B and C show elastic matrix amounts deposited in cell cultures on an absolute and cell number-normalized basis, respectively. Total matrix elastic matrix protein amounts were significantly higher in both the derived phenotypes compared to RASMCs ($p<0.001$), but lower compared to BM-MSCs ($p<0.004$). However, on a cell-normalized basis, elastic matrix production by the RASMCs was significantly higher than by the cBM-SMCs, rBM-SMCs, and BM-MSCs ($p<0.001$). There were no differences in elastic matrix synthesis on a per cell basis between cBM-SMCs and rBM-SMCs.

Desmosine crosslink content

As indicated in Figure 4D, on a protein content normalized basis, desmosine crosslink content in cBM-SMC cultures was significantly higher than in other cases ($p<0.003$).

Collagen matrix deposition

Results of a hydroxyproline assay (Fig. 5) indicated little collagen matrix in RASMC cultures and significantly higher amounts in all other tested cell types ($p\leq0.001$); there were no significant differences in collagen synthesis between the two derived SMC subtypes and between these cultures and BM-MSC cultures. On a per cell normalized basis, collagen content was again higher in the differentiated SMC cultures compared to RASMCs ($p<0.001$) and BM-MSCs ($p<0.02$), but not different between cBM-SMCs and rBM-SMCs. BM-MSCs also had significantly higher collagen/cell compared to RASMCs ($p=0.01$).

MMP-2 and MMP-9 protein synthesis

Synthesis of MMP-2 (72 kDa, 66 kDa isoforms) and MMP-9 (82 kDa, 72 kDa isoforms) proteins were measured using ELISA and results are shown in Figure 6. MMP-2 protein synthesis was significantly higher in cBM-SMC cultures compared to all other cell types ($p\leq0.003$), which is consistent with Western blot results. rBM-SMCs also generated significantly higher amounts of MMP-2 protein compared to RASMCs ($p=0.002$) and BM-MSCs ($p=0.038$), but less so than the cBM-SMCs ($p=0.003$). MMP-9 protein was not expressed in RASMC and cBM-SMC cultures. MMP-9 synthesis by rBM-SMCs was significantly higher ($p\leq0.005$) compared to all other cell types.

Elastic matrix ultrastructure

TEM (Fig. 7) showed presence of a homogenously dense matrix composed of forming elastic fibers in the cBM-SMC cultures, and noticeably less dense elastic matrix deposition in the rBM-SMC cultures. The forming fibers comprised both essential components, namely the microfibrillar prescaffold (white arrows) on to which crosslinked amorphous elastin coacervates (red arrows) were deposited. In contrast, elastic fiber deposition was poor in RASMC and EaRASMC cultures and only sporadic, amorphous elastin clumps were seen.

Discussion

In this project, we have sought to determine if continued provision of differentiation conditions (fibronectin substrate, TGF-β, and PDGF-ββ) is essential to maintain the phenotype and matrix synthesis properties of BM-SMCs during their propagation in two-dimensional culture, before delivery *in vivo*. To confirm differentiation of BM-MSCs

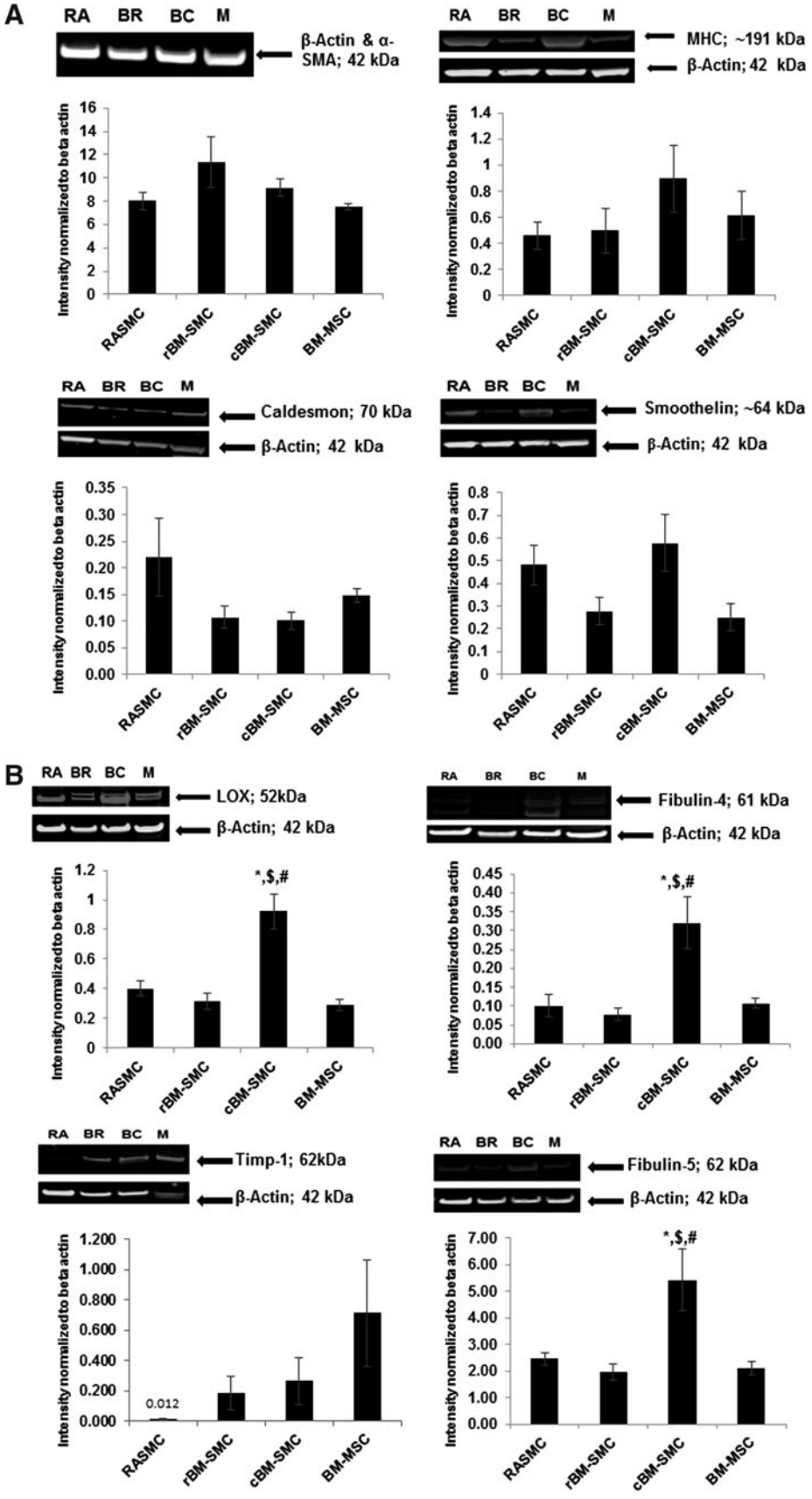

FIG. 2. Western blot analysis for expression of SMC marker proteins **(A)** shows no significant differences between the four cell types. Western blot analysis for expression of key elastic matrix assembly proteins **(B)** indicates significantly higher LOX, fibulin-4, and fibulin-5 expression by cBM-SMCs, whereas no significant differences were found among the four cell types in TIMP-1 expression. *, $, and # indicate statistical significance compared to RASMCs, cBM-SMCs, and BM-MSCs, respectively, deemed for $p < 0.05$. RA, BR, BC, and M in the blot represent RASMCs, rBM-SMCs, cBM-SMCs, and BM-MSCs, respectively. After analysis of the bands, the images of the blots were brightness/contrast enhanced, as shown, for easier visualization in print.

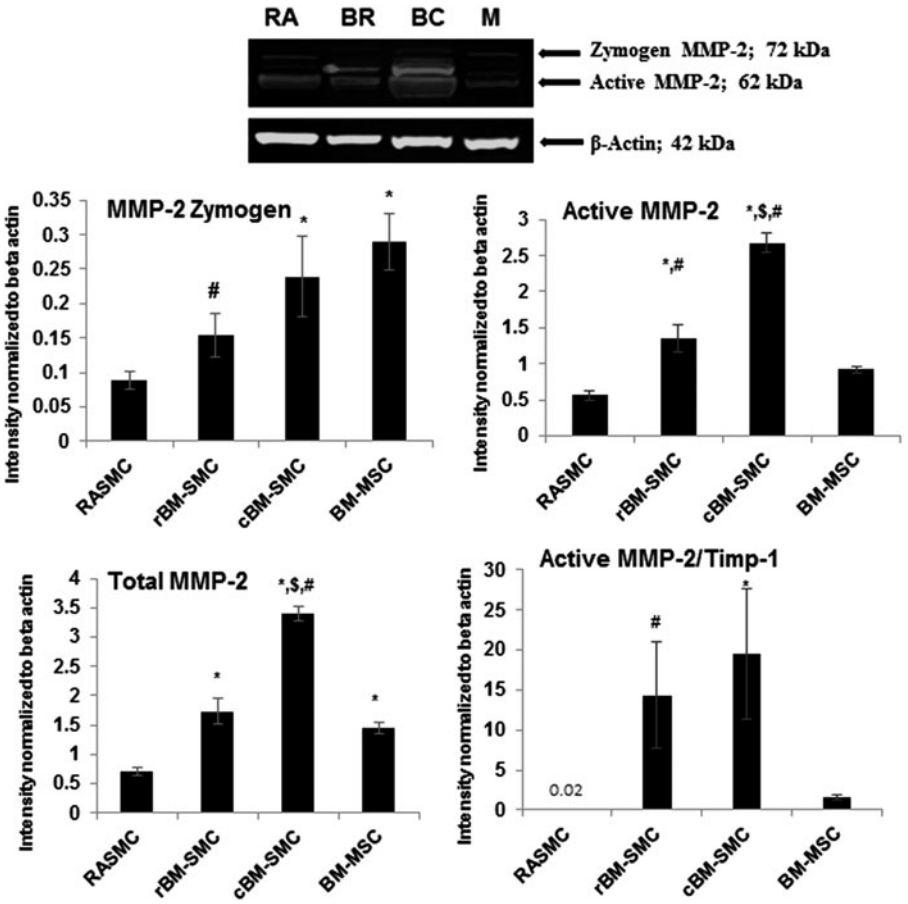

FIG. 3. Western blot analysis for MMP-2 protein expression. The figure compares expression of MMP-2 zymogen, active MMP-2, and total MMP-2 by all four cell types as also measures of net proteolytic activity, that is, ratios of active MMP-2 to TIMP-1. *, $, and # indicate statistical significance compared to RASMCs, cBM-SMCs, and BM-MSCs, respectively, deemed for $p < 0.05$. After analysis of band intensities, the blot images were brightness/contrast enhanced as shown for easier visualization in print. RA, BR, BC, and M in the blot represents RASMCs, rBM-SMCs, cBM-SMCs, and BM-MSCs, respectively. MMPs, matrix metalloproteases.

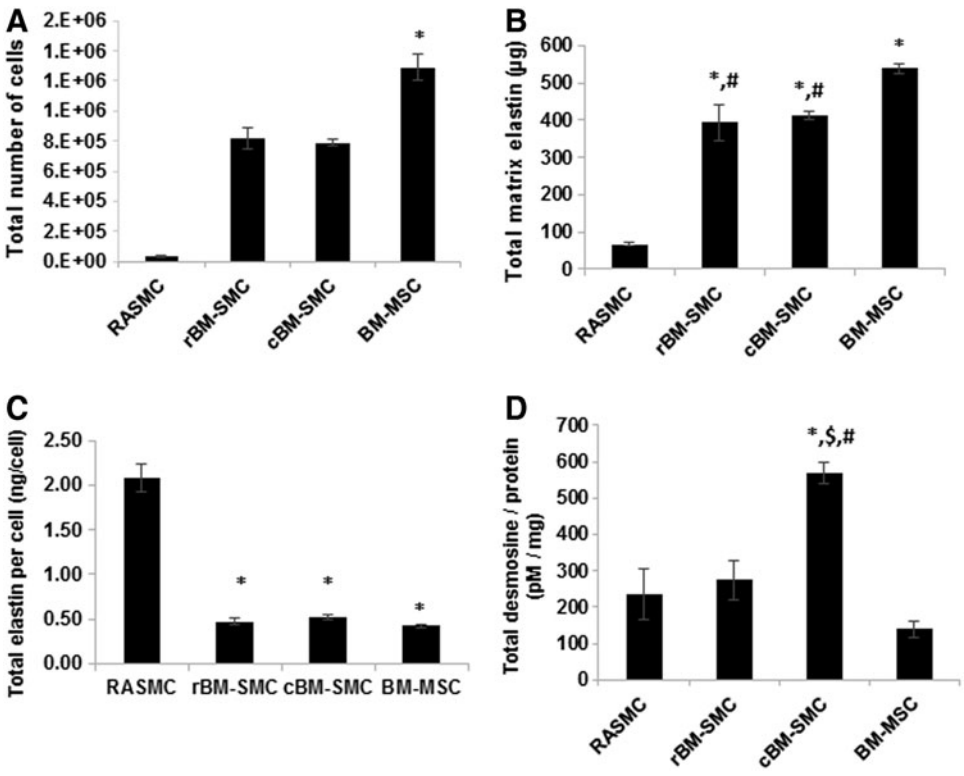

FIG. 4. Differences between derived SMC subtypes and RASMC and BM-MSC controls in cell proliferation **(A)**, elastic matrix amounts on a total **(B)** and a cell count-normalized **(C)** basis, and desmosine crosslink amounts within the matrix, shown normalized to total protein content in the respective cell layers **(D)**. In all cases, 30,000 cells were seeded per well in a 6-well plate and cultured for 21 days before analysis for cell counts, elastin, and desmosine. *, $, and # indicate statistical significance compared to RASMCs, cBM-SMCs, and BM-MSCs, respectively, deemed for $p < 0.05$.

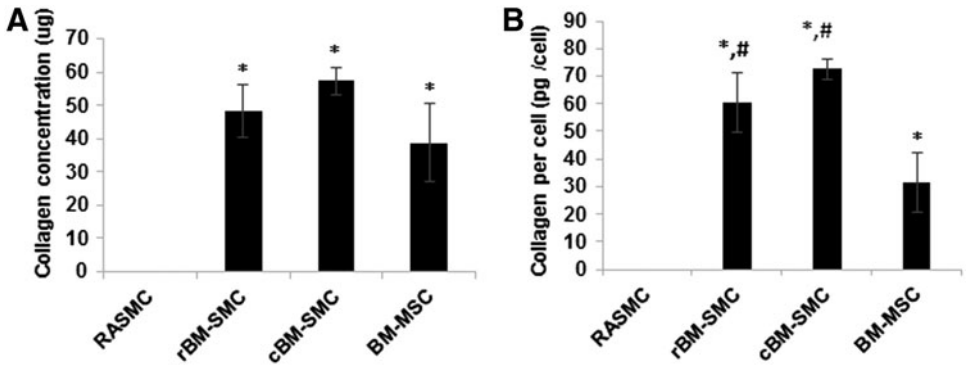

FIG. 5. Cell type-specific differences in collagen synthesis measured using a hydroxyproline assay shown in absolute amounts **(A)** and amounts on a cell count-normalized basis **(B)**. No significant differences were found between the two derived cell types; however, cell normalized collagen content was higher in both of them compared to RASMCs and BM-MSCs. * and # indicate statistical significance compared to RASMCs and BM-MSCs, respectively, deemed for $p < 0.05$.

into SMCs, we investigated the expression of SMC phenotypic markers by our generated BM-SMC culture groups. While SMA is expressed by the SMCs even early in their differentiation, caldesmon is expressed in the mid-stage of differentiation. On the other hand, smoothelin and MHC are markers that are exclusively expressed by contractile SMCs.[13] The RT-PCR results showed the derived cells to be similar to healthy RASMCs in exhibiting contractile SMC markers, but to not be terminally differentiated. The cBM-SMCs robustly expressed *ACTA2*, but not *MYH11*, suggesting that they are not terminally differentiated as are the RASMCs and SMCs in native vessels, but are rather of an early or intermediate SMC phenotype. *SMTN* and *MYH11* expression being similar between the two derived cell types, higher *CALD1* expression by the BM-SMCs points to their relatively higher maturation versus the cBM-SMCs.

Despite the differences in gene expression profiles, expression of SMC marker proteins was not statistically different between the cell groups, quite possibly due to the Western blot analysis being less precise and data hence generated with relatively large variability. Regardless, these Western blot data confirm our derived cell types to be SMC like. The limited expression of these same SMC markers by the undifferentiated BM-MSCs on the other hand has been described in literature.[27]

Superior elastogenic properties are critical to selection of cells toward application to AAA wall repair. One of the major players in regulation of elastin homeostasis and vessel remodeling is LOX, a copper-dependent amine oxidase that enables elastin crosslinking and consequent stabilization. LOX downregulation is thought to have a central role in the instability of plaque leading to destructive remodeling, like it takes place in case of aneurysm.[28] We found significantly higher *LOX* gene expression and protein synthesis in cBM-SMC cultures than in all other cell groups, suggesting a better crosslinked and proteolysis-resistant elastic matrix in those cultures. This may be due to the continued presence of TGF-β1, which is known to upregulate both LOX gene expression and protein synthesis.[29] Fibronectin in the cell substrate is known to bind LOX and LOXL1 proenzymes, and activates BMP-1, and through the auspices of the latter, proteolytically cleave the proenzymes to release active LOX enzyme,[30,31] increasing the LOX activity.

Another important measure of elastin crosslinking is desmosine, which is a tetrafunctional amino acid that links elastin molecules. Desmosine content was significantly

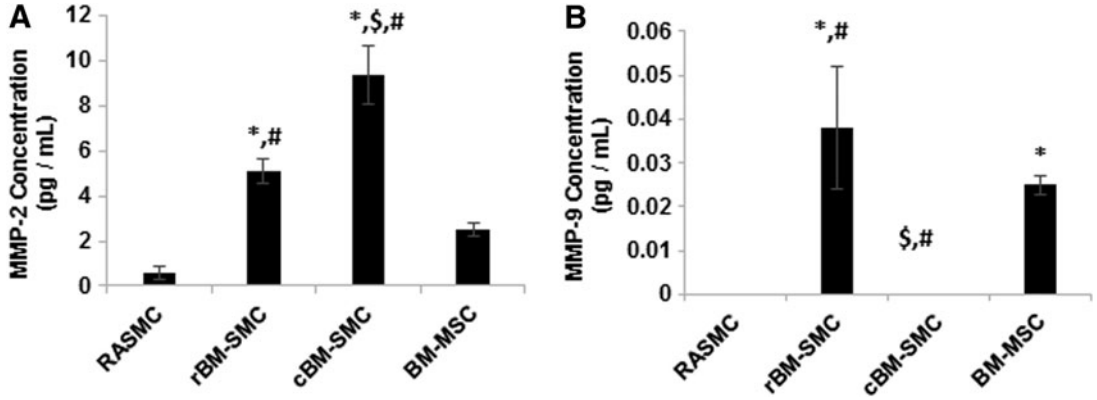

FIG. 6. Protein concentrations of MMP-2 **(A)** and MMP-9 **(B)** measured in cell layers using ELISA. Results show significantly higher MMP-2 protein amounts in cBM-SMC cultures compared to rBM-SMC, RASMC, and BM-MSC cultures, and significantly lower MMP-9 protein amounts relative to rBM-SMC and BM-MSC cultures. *, $, and # indicate statistical significance compared to RASMCs, cBM-SMCs, and BM-MSCs, respectively, deemed for $p < 0.05$.

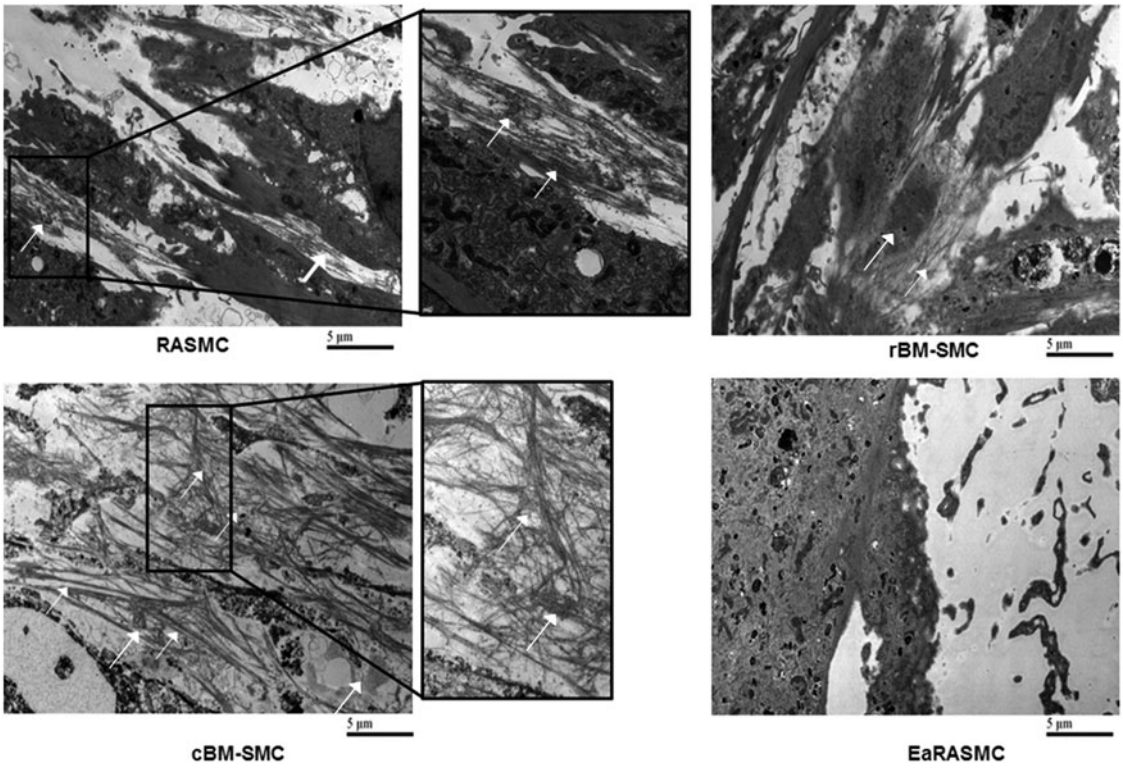

FIG. 7. Transmission electron micrographs showing significantly greater density of forming elastic fibers in cBM-SMC cultures, and less so in rBM-SMC cultures relative to RASMC cultures. The elastic fibers were composed of fibrillin microfibrils (*white arrows*) laid down as a prescaffold onto which amorphous elastin (*red arrows*) was deposited and crosslinked. The RASMC cultures contained mainly amorphous elastin deposits. Very few amorphous elastin deposits and no fiber-like structures were seen in EaRASMC cultures.

higher in the cBM-SMC cultures than in the other culture groups, likely as a result of higher LOX synthesis/activity. In addition, fibronectin facilitates deposition of fibrillin-1 microfibrils,[32,33] which are a prerequisite to initiate elastic matrix/fiber assembly that is consistent with increased elastic matrix fiber deposition in cBM-SMC cultures. More specifically, fibrillin-1 is deposited as a prescaffold upon which elastin is deposited and coacervates and extends to form a matrix fiber.[34,35] Fibrillin-1 expression by cBM-SMCs is likely increased in the presence of exogenous TGF-β.[36]

Fibulins 4 and 5 coacervate tropoelastin to facilitate their integration with fibrillin-1 microfibrils for crosslinking by either LOX (fibulin-4)[37] or its homologue LOXL1 (Fibulin-5),[38,39] to which they also bind to promote elastic fiber assembly.[40] In fact, a mutation in the homozygous fibulin-4 has been implicated in AAA pathophysiology.[41] In our study, gene expression and protein synthesis of both fibulins 4 and 5 were the highest in cBM-SMC cultures, followed by the rBM-SMC cultures. While fibulin-4 facilitates LOX binding to both fibrillin-1 and tropoelastin nuclei and processes it to an enzymatically active form,[37] fibulin-5 similarly regulates the LOX isoform, LOXL1, expressed typically in adult cells.[42] The higher expression of fibulins 4 and 5 in cBM-SMC cultures thus implies improved elastic matrix deposition and fiber formation, which was the case. In this context, our study outcomes were also consistent with our earlier data in showing that elastin expression by cBM-SMCs is significantly higher than expression by BM-MSCs and RASMCs.[15]

On the other hand, elastic matrix synthesis by rBM-SMCs was below levels in BM-MSC cultures, which may be related to the absence of any supplemented growth factor, although further investigation is warranted. However, no differences in elastic matrix deposition were noted on a per cell basis between the derived SMC types, which were higher than in BM-MSC cultures, and in the case of cBM-SMCs, similar to the RASMCs. This discrepancy between the PCR data and Fastin assay data can be attributed to the fact that elastic matrix assembly not only depends on posttranscriptional processes resulting in synthesis of elastin precursors but also a complex hierarchical process of fiber assembly involving parallel or sequential involvement of numerous other elastic fiber assembly proteins (LOX, fibulins, fibrillins, and fibronectin), several of which were upregulated in cBM-SMC cultures versus the other cell types. In addition, total elastic matrix amounts generated by cBM-SMCs are significantly greater than RASMCs due to their more rapid proliferation postseeding.

Since the benefits of a matrix regenerative cell therapy, as we propose, ultimately depends upon that total amount of new elastic matrix generated, both our derived SMC types may be deemed superior to the RASMCs, although greater expression of elastic fiber homeostasis proteins by the cBM-SMCs points to their likely superior elastogenic properties versus rBM-SMCs. Supporting these results, TEM (Fig. 7) showed robust deposition of a fibrous elastic matrix (white arrows) in the extracellular space within cBM-SMC

cultures, less so in rBM-SMC cultures, and only sporadic deposition of fibrous elastin and amorphous elastin clumps (red arrows) in RASMC and EaRASMC cultures. Our data in Figures 2–5 also suggest that elastic fiber formation by BM-MSCs is likely to be poor due to the much lower expression of key proteins involved in elastic fiber assembly proteins, although total elastic matrix deposition itself is high due to high proliferative capacity of these cells. This, in addition to the lack of their proelastogenic effects on aneurysmal SMCs[14,15], renders BM-MSCs less efficacious for cell therapy aimed at regenerating elastic matrix.

While our data collectively suggest that phenotype influences elastic matrix assembly properties of BM-MSC-derived SMCs, no differences were noted in collagen matrix deposition between the cBM-SMCs and rBM-SMCs, which were significantly higher than that in RASMC cultures. In the latter, collagen amounts were below the limit of detection, which can be at least, in part, attributed to low cell numbers owing to the intrinsically poor proliferative capacity of RASMCs. While MMP-2 protein synthesis measured by Western blot and ELISA was higher in cBM-SMC cultures, MMP-9 was not, consistent with gene expression trends. The findings as to low expression of MMP-9 are also consistent with prior observations by our group.[14,15,43] This may be owed to poor constitutive expression of MMP-9 by SMCs in culture, which is well documented.[44] Since MMP-2 and MMP-9 are countered by TIMP-1, MMP-2/TIMP-1 ratios protein ratios were compared between the culture groups. The MMP-2/TIMP-1 ratios observed in the cBM-SMC cultures were higher versus the RASMCs, which might be considered a suboptimal outcome. This could be possibly attributed to the pro-MMP-2 effects of the TGF-β at certain doses,[45] specially in the absence of its sequestration in the absence of a 3D ECM.

However, we have shown in a parallel study, results of which are being published separately, that subsequently introducing these propagated cBM-SMCs into a 3D collagenous tissue milieu in the absence of TGF-β1 and PDGF-ββ causes significant attenuation of MMP-2. This might be related to their release of more paracrine signaling molecules, some with antiproteolytic effects in 3D culture[20,26] or alternately, the ability of the 3D ECM to sequester the endogenous TGF-β to prevent its activation and possible stimulation of MMP-2. Regardless of this, cBM-SMCs can be deemed the superior derived phenotype, owing to their lack of MMP-9 expression, unlike the rBM-SMCs.

Conclusions

While we have separately demonstrated that our differentiated cBM-SMCs maintain the proelastogenic and antiproteolytic benefits when introduced into a de-elasticized collagen-rich tissue milieu and thereafter maintained in the absence of differentiation growth factors, this study shows that propagation of the differentiated BM-SMCs in an *in vitro* 2D culture must necessarily be performed in the continued presence of differentiation culture conditions to maintain their phenotype. The results have vital implications to successful generation of large cBM-SMC populations for subsequent use in cell therapy for AAAs.

Acknowledgments

The authors acknowledge research funding for this project from the National Science Foundation (1508642) and National Institutes of Health (HL132856), awarded to A.R. This work utilized the FEI Tecnai G2 Spirit transmission electron microscope that was purchased with funding from National Institutes of Health SIG grant 1S10RR031536-01. The authors thank Ms. Mei Lin of the Lerner Research Institute Imaging Core for her assistance with TEM.

Disclosure Statement

No competing financial interests exist.

References

1. Sakalihasan, N., Delvenne, P., Nusgens, B.V., Limet, R., and Lapière, C.M. Activated forms of MMP2 and MMP9 in abdominal aortic aneurysms. J Vasc Surg **24,** 127, 1996.
2. Petersen, E., Gineitis, A., Wågberg, F., and Ängquist, K.A. Activity of matrix metalloproteinase-2 and –9 in abdominal aortic aneurysms. Relation to size and rupture. Eur J Vasc Endovasc Surg **20,** 457, 2000.
3. Stabler, T., Renner, J.B., Schwartz, T.A., *et al.* NIH public access. J Immunol **17,** 772, 2010.
4. Mao, N., Gu, T., Shi, E., Zhang, G., Yu, L., and Wang, C. Phenotypic switching of vascular smooth muscle cells in animal model of rat thoracic aortic aneurysm. Interact Cardiovasc Thorac Surg **21,** 62, 2015.
5. Aggarwal, S., Qamar, A., Sharma, V., and Sharma, A. Abdominal aortic aneurysm: a comprehensive review. Exp Clin Cardiol **16,** 11, 2011.
6. Eliason, J.L., and Upchurch, G.R. Endovascular abdominal aortic aneurysm repair. Circulation **117,** 1738, 2008.
7. England, A., and Mc Williams, R. Endovascular aortic aneurysm repair (EVAR). Ulster Med J **82,** 3, 2013.
8. Yamawaki-Ogata, A., Hashizume, R., Fu, X.-M., Usui, A., and Narita, Y. Mesenchymal stem cells for treatment of aortic aneurysms. World J Stem Cells **6,** 278, 2014.
9. Bashur, C.A., Rao, R.R., and Ramamurthi, A. Perspectives on stem cell-based elastic matrix regenerative therapies for abdominal aortic aneurysms. Stem Cells Transl Med **2,** 401, 2013.
10. Swaminathan, G., Gadepalli, V.S., Stoilov, I., Mecham, R.P., Rao, R.R., Ramamurthi, A. Pro-elastogenic effects of bone marrow mesenchymal stem cell-derived smooth muscle cells on cultured aneurysmal smooth muscle cells. J Tissue Eng Regen Med 4, 524, 2014.
11. Owens, G.K. Regulation of differentiation of vascular smooth muscle cells. Physiol Rev **75,** 487, 1995.
12. Stegemann, J.P., Hong, H., Nerem, R.M., and Jan, P. Mechanical, biochemical, and extracellular matrix effects on vascular smooth muscle cell phenotype. J App Physiol **98,** 2321, 2005.
13. Rensen, S.S.M., Doevendans, P.A.F.M., and van Eys, G.J.J.M. Regulation and characteristics of vascular smooth muscle cell phenotypic diversity. Neth Heart J **15,** 100, 2007.
14. Swaminathan, G., Stoilov, I., Broekelmann, T., Mecham, R., and Ramamurthi, A. Phenotype-based selection of bone marrow mesenchymal stem cell-derived smooth muscle cells for elastic matrix regenerative repair in abdominal aortic aneurysms. J Tissue Eng Regen Med **11,** 979, 2017.
15. Swaminathan, G., Gadepalli, V.S., Stoilov, I., Mecham, R.P., Rao, R.R., and Ramamurthi, A. Pro-elastogenic effects of bone marrow mesenchymal stem cell-derived smooth muscle

cells on cultured aneurysmal smooth muscle cells. J Tissue Eng Regen Med **4,** 524, 2014.
16. Kothapalli, C.R., and Ramamurthi, A. Induced elastin regeneration by chronically activated smooth muscle cells for targeted aneurysm repair. Acta Biomater **6,** 170, 2010.
17. Pfaffl, M.W. A new mathematical model for relative quantification in real-time RT-PCR. Nucleic Acids Res **29,** 45e, 2001.
18. Sivaraman, B., Swaminathan, G., Moore, L., *et al.* Magnetically-responsive, multifunctional drug delivery nanoparticles for elastic matrix regenerative repair. Acta Biomater **52,** 171, 2016.
19. Starcher, B. A ninhydrin-based assay to quantitate the total protein content of tissue samples. Anal Biochem **292,** 125, 2001.
20. Venkataraman, L., and Ramamurthi, A. Induced elastic matrix deposition within three-dimensional collagen scaffolds. Tissue Eng Part A **17,** 2879, 2011.
21. Actin, B., Care, C., and Us, A. Beta Actin and GAPDH: The Importance of Loading Controls. https://www.novusbio.com/antibody-news/antibodies/the-importance-of-beta-actin-and-gapdh-loading-controls. (last accessed January 6, 2018).
22. An, Z., Qiao, F., Lu, Q., *et al.* Interleukin-6 downregulated vascular smooth muscle cell contractile proteins via ATG4B-mediated autophagy in thoracic aortic dissection. Heart Vessels **32,** 1523, 2017.
23. Crosas-Molist, E., Meirelles, T., López-Luque, J., *et al.* Vascular smooth muscle cell phenotypic changes in patients with marfan syndrome. Arterioscler Thromb Vasc Biol **35,** 960, 2015.
24. Shi, X., DiRenzo, D., Guo, L.W., *et al.* TGF-β/Smad3 stimulates stem cell/developmental gene expression and vascular smooth muscle cell de-differentiation. PLoS One **9,** e103796, 2014.
25. Mao, N., Gu, T., Shi, E., Zhang, G., Yu, L., and Wang, C. Phenotypic switching of vascular smooth muscle cells in animal model of rat thoracic aortic aneurysm. Interact Cardiovasc Thorac Surg **21,** 62, 2015.
26. Gacchina, C.E., and Ramamurthi, A. Impact of pre-existing elastic matrix on TGF??1 and HA oligomer-induced regenerative elastin repair by rat aortic smooth muscle cells. J Tissue Eng Regen Med **5,** 85, 2011.
27. Liu, Y., Deng, B., Zhao, Y., Xie, S., and Nie, R. Differentiated markers in undifferentiated cells: expression of smooth muscle contractile proteins in multipotent bone marrow mesenchymal stem cells. Dev Growth Differ **55,** 591, 2013.
28. Rodríguez, C., Martínez-González, J., Raposo, B., Alcudia, J.F., Guadall, A., and Badimon, L. Regulation of lysyl oxidase in vascular cells: lysyl oxidase as a new player in cardiovascular diseases. Cardiovasc Res **79,** 7, 2008.
29. Min, C., Kirsch, K.H., Zhao, Y., *et al.* The tumor suppressor activity of the lysyl oxidase propeptide reverses the invasive phenotype of Her-2/neu-driven breast cancer. Cancer Res **67,** 1105, 2007.
30. Fogelgren, B., Polgár, N., Szauter, K.M., *et al.* Cellular fibronectin binds to lysyl oxidase with high affinity and is critical for its proteolytic activation. J Biol Chem **280,** 24690, 2005.
31. Xiao, Q., and Ge, G. Lysyl oxidase, extracellular matrix remodeling and cancer metastasis. Cancer Microenviron **5,** 261, 2012.
32. Kinsey, R., Williamson, M.R., Chaudhry, S., *et al.* Fibrillin-1 microfibril deposition is dependent on fibronectin assembly. J Cell Sci **121,** 2696, 2008.
33. Mosher, D.F. Assembly of fibronectin into extracellular matrix. Curr Opin Struct Biol **3,** 214, 1993.
34. Wagenseil, J.E., and Mecham, R.P. New insights into elastic fiber assembly. Birth Defects Res C Embryo Today Rev **81,** 229, 2007.
35. Clarke, A.W., Wise, S.G., Cain, S.A., Kielty, C.M., and Weiss, A.S. Coacervation is promoted by molecular interactions between the PF2 segment of fibrillin-1 and the domain 4 region of tropoelastin. Biochemistry **44,** 10271, 2005.
36. Lorena, D., Darby, I.A., Reinhardt, D.P., Sapin, V., Rosenbaum, J., and Desmoulière, A. Fibrillin-1 expression in normal and fibrotic rat liver and in cultured hepatic fibroblastic cells: modulation by mechanical stress and role in cell adhesion. Lab Invest **84,** 203, 2004.
37. Horiguchi, M., Inoue, T., Ohbayashi, T., *et al.* Fibulin-4 conducts proper elastogenesis via interaction with cross-linking enzyme lysyl oxidase. Proc Natl Acad Sci U S A **106,** 19029, 2009.
38. Drewes, P.G., Yanagisawa, H., Starcher, B., *et al.* Pelvic organ prolapse in fibulin-5 knockout mice. Am J Pathol **170,** 578, 2007.
39. Northington, G.M. Fibulin-5: two for the price of one maintaining pelvic support. J Clin Invest **121,** 1688, 2011.
40. Chalovich, J.M., and Eisenberg, E. NIH public access. Biophys Chem **257,** 2432, 2005.
41. Evans, J.A. Diaphragmatic defects and limb deficiencies—taking sides. Am J Med Genet A **143A,** 2106, 2007.
42. Choudhury, R., McGovern, A., Ridley, C., *et al.* Differential regulation of elastic fiber formation by fibulin-4 and –5. J Biol Chem **284,** 24553, 2009.
43. Gacchina, C., Brothers, T., and Ramamurthi, A. Evaluating smooth muscle cells from CaCl2-induced rat aortal expansions as a surrogate culture model for study of elastogenic induction of human aneurysmal cells. Tissue Eng Part A **17,** 1945, 2011.
44. Crowther, M., Goodall, S., Jones, J.L., Bell, P.R., and Thompson, M.M. Increased matrix metalloproteinase 2 expression in vascular smooth muscle cells cultured from abdominal aortic aneurysms. J Vasc Surg **32,** 575, 2000.
45. Kim, E.S., Sohn, Y.W., and Moon, A. TGF-β-induced transcriptional activation of MMP-2 is mediated by activating transcription factor (ATF)2 in human breast epithelial cells. Cancer Lett **252,** 147, 2007.

Address correspondence to:
Anand Ramamurthi
Department of Biomedical Engineering
Cleveland Clinic
9500 Euclid Avenue
Cleveland, OH 32901

E-mail: ramamua@ccf.org

Received: April 28, 2017
Accepted: December 19, 2017
Online Publication Date: February 1, 2018